OPTOELECTRONICS AND ADVANCED MATERIALS – RAPID COMMUNICATIONS Vol. 6, No. 5-6, May - June 2012, p. 547 - 550

Influence of Yb^{3+} co-doping on Er^{3+} up-conversion emission in $NaYF_4:Er^{3+}$ phosphor under 808 nm excitation

LINGLING JIANG[a], HUABING ZHANG[a], SIGUO XIAO[a,b,*], XIANGLIANG YANG[a,b], JIANWEN DING[a,b]
[a]Institute for Nanophysics and Rare-earth Luminescence, Xiangtan University, Xiangtan 411105, Hunan, China
[b]Key Laboratory of Low Dimensional Materials & Application Technology, Xiangtan University, Xiangtan, Hunan 411105, P.R. China

Intense green and red emissions are observed in Er^{3+} singly-doped and Er^{3+}/Yb^{3+}-codoped $NaYF_4$ phosphors under 808nm excitation. Co-doped Yb^{3+} ions reduce Er^{3+} up-conversion emission at low Er^{3+} doping concentration, while they enhance the up-conversion emission at relatively high Er^{3+} concentration. A competitive energy transfer mechanism between $Yb^{3+} \rightarrow Er^{3+}$ and $Er^{3+} \rightarrow Yb^{3+}$ is proposed to explain the Yb^{3+} dependent Er^{3+} up-conversion behavior.

(Received February 21, 2012; accepted June 6, 2012)

Keywords: Er^{3+}, Yb^{3+}, Up-conversion, Energy transfer

1. Introduction

Recently, exploration on infrared-to-visible frequency up-conversion in rare-earth (RE) doped materials has become much more significant because of its potential applications in visible up-conversion lasers, undersea communication, medical diagnostics, high density optical memories, solid-state color displays [1-13], and so on. Among rare-earth ions for luminescence centers, Er^{3+} exhibits excellent up-conversion performance because of the intermediate levels $^4I_{11/2}$ (about 10219 cm^{-1}) and $^4I_{9/2}$ (about 12378 cm^{-1}). These levels can be conveniently populated by commercial low-cost high-power near-infrared laser diodes, subsequently performing blue, green, and red up-conversion emissions [14-19]. Er^{3+} up-conversion emission can be performed under both 808nm and 980nm excitation, many studies have showed that Yb^{3+} ion can be used as a sensitizer for Er^{3+} up-conversion emission under 980nm excitation [20-25]. S. Inoue et al reported the enhancement of Yb^{3+} on Er^{3+} up-conversion under 808nm excitation [26]. In our previous work [27], it was found that up-conversion under 812nm excitation tended to decrease in $Ba_2ErF_7:Yb^{3+}$ by the introduction of Yb^{3+}, due to so much high Er^{3+} concentration.

In this work, we investigate the effect of Yb^{3+} co-doped on Er^{3+} up-conversion emission intensity at different Er^{3+} concentrations in $NaYF_4:Er^{3+}$ under 808nm excitation. It's found that up-conversion emission of Er^{3+} can be enhanced by co-doping with Yb^{3+} ions in $NaYF_4:Er^{3+}$ powder at proper Er^{3+} concentration. A competitive energy transfer mechanism between $Yb^{3+} \rightarrow Er^{3+}$ and $Er^{3+} \rightarrow Yb^{3+}$ is proposed to explain the Yb^{3+} dependent up-conversion behavior.

2. Experimental

The samples were prepared by a solid-state reaction method. The starting materials were reagent grade 99.9% purity NaF, 99.9% purity YF_3, 99.999% purity ErF_3 and 99.999% purity YbF_3. The samples were synthesized according to the molar composition of $NaY_{1-x-y}Yb_xEr_yF_4$ (y=0.5, 5 mol%, x=0, 5, 8, 11, 14, 17 mol%). Details of $NaYF_4$ preparation procedures had been described in our previous work [28].

The X-ray diffraction patterns of the samples were measured on a D-8 advance equipment providing with Cu tube with K_α radiation of 1.54056 Å, scanning in the 2Θ range of 10° to 80° with 0.01° increments and 6s sweep time. The up-conversion spectra excited by an 808nm diode laser were obtained by the R-500 Spectrophotometer with resolution limit of 0.45 cm^{-1} made by Japan Spectroscopic CO, LTD. The excitation laser beam was focused on the samples using a focal length lens of 3 cm and the spot size of 1 mm was obtained. The samples were pressed into thin flat disks with the same size (diameter D = 1 cm) and smooth surface for measurement. The signal of luminescence was detected at the angle of 90° with the incident beam. All the measurements were performed at room temperature.

3. Results and discussions

Fig. 1 shows representative X-ray diffraction patterns of $NaY_{1-x-y}Yb_xEr_yF_4$ (x=0, 8, 14 mol%, y=5 mol%). The patterns indicate that the samples have been synthesized into pure hexagonal-$NaYF_4$, according to the standard X-ray diffraction JCPDS 16-0334.

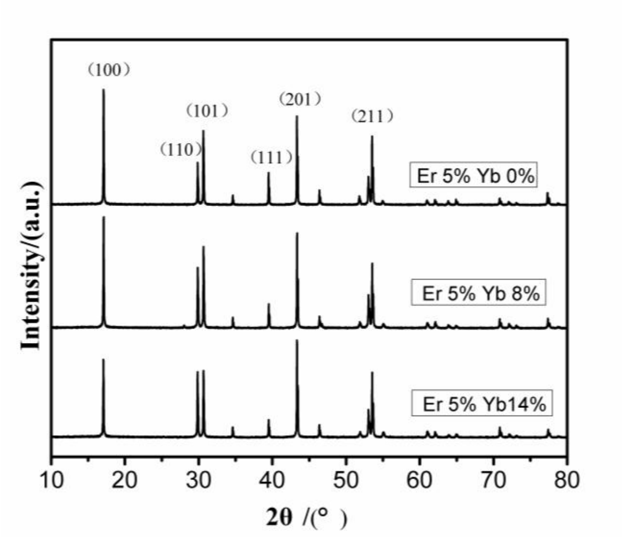

Fig. 1. Powder XRD patterns of $NaY_{1-x-y}Yb_xEr_yF_4$ *(x=0, 8, 14 mol%, y=5 mol%).*

Up-conversion emission spectra of Er^{3+} singly-doped $NaYF_4$ is shown in Fig. 2. Eight emission bands of Er^{3+} are observed, centered at 389, 408, 455, 492, 505, 525, 542 and 655nm, which are assigned to $^4G_{11/2} \rightarrow {}^4I_{15/2}$, $^2H_{9/2} \rightarrow {}^4I_{15/2}$, $^4F_{5/2} \rightarrow {}^4I_{15/2}$, $^4F_{7/2} \rightarrow {}^4I_{15/2}$, $^4G_{11/2} \rightarrow {}^4I_{13/2}$, $^2H_{11/2} \rightarrow {}^4I_{15/2}$, $^4S_{3/2} \rightarrow {}^4I_{15/2}$ and $^4F_{9/2} \rightarrow {}^4I_{15/2}$ transitions respectively [29-31]. The most intense band is the green emission $^4S_{3/2} \rightarrow {}^4I_{15/2}$, and the secondary one is the red emission $^4F_{9/2} \rightarrow {}^4I_{15/2}$. Other emissions are much weaker than the two.

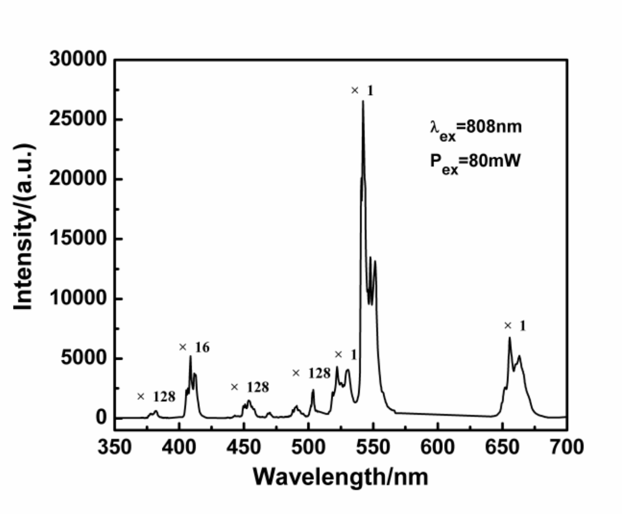

Fig. 2. Up-conversion emission spectra of Er^{3+}*-doped* $NaYF_4$ *phosphor under 808nm excitation.*

Fig. 3 presents the dependence of up-conversion luminescence intensity on Er^{3+} concentration. With the increase of Er^{3+} concentration from 1 mol% to 6 mol%, the green emission firstly increases and then decreases, with an optimum Er^{3+} concentration at 5 mol%. Thus in order to investigate the influence of Yb^{3+} concentration on up-conversion emission of Er^{3+}, two typical Er^{3+} concentrations, 0.5 mol% and 5 mol%, are selected to investigate the Yb^{3+} dependent Er^{3+} up-conversion behavior.

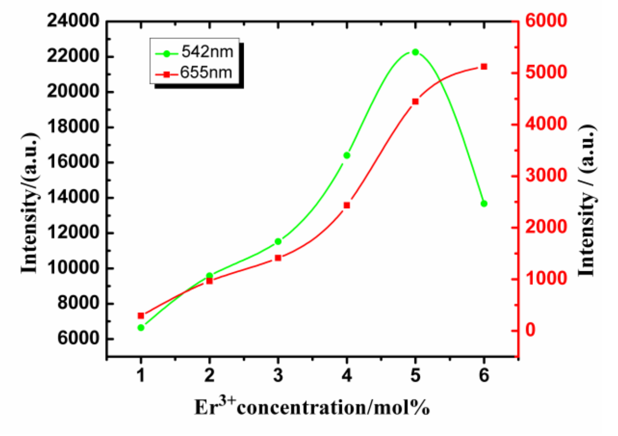

Fig. 3. Dependence of up-conversion luminescence intensity on Er^{3+} *concentrations under 808nm excitation.*

Fig. 4 shows Er^{3+} emission intensities as functions of Yb^{3+} concentrations under 808nm excitation. For the samples at Er^{3+} concentration of 0.5 mol%, increasing Yb^{3+} concentration from 0 to 14 mol%, the green and red emissions decrease drastically and then increase slightly. However, at any concentration of Yb^{3+}, up-conversion intensities of the co-coped samples are much weaker than that of Er^{3+} singly-doped samples. This indicates that Yb^{3+} quenches Er^{3+} up-conversion when Er^{3+} concentration is 0.5 mol%. For the samples at 5 mol% Er^{3+}, the Yb^{3+} dependent behavior on the red emission is similar to that of 0.5 mol% Er^{3+} doped ones. It decreases at first and then tends to increase. When Yb^{3+} concentration reaches to 14 mol%, the red emission for the co-doped sample is stronger than the Er^{3+} singly doped counterpart. On the other hand, the green emission always increases upon increasing Yb^{3+} concentration. It is noteworthy that the green emission for the samples co-doped with different concentrations of Yb^{3+} is always stronger than that of Er^{3+} singly-doped counterpart. Especially, at Er^{3+} concentration of 5 mol%, 14 mol% Yb^{3+} makes the green and red emissions enhanced nearly two times compared with the Er^{3+} singly-doped samples. Concentration quenching only occurs when Yb^{3+} concentration is higher than 14 mol%. It suggests that a suitable Yb^{3+} concentration can really improve the up-conversion for the samples with 5 mol% Er^{3+}.

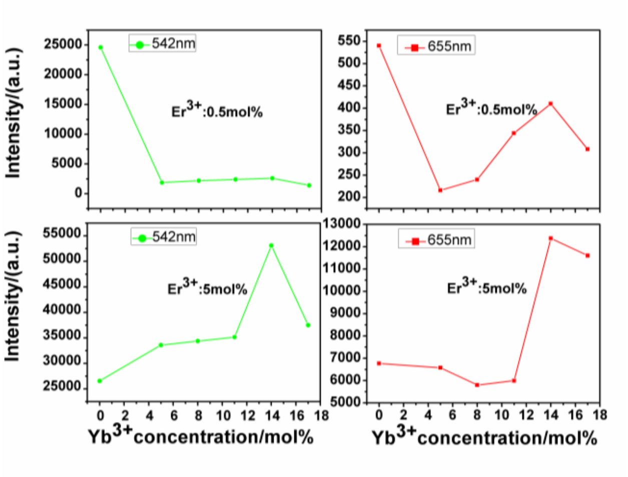

Fig. 4. Er^{3+} emission intensity as functions of Yb^{3+} concentrations for the samples with 0.5 mol% and 5 mol% Er^{3+}.

The dependence of red and green emission intensities on the infrared excitation power in $NaYF_4$:0.5 mol% Er^{3+}, 14 mol% Yb^{3+} and $NaYF_4$:5 mol% Er^{3+}, 14 mol% Yb^{3+} are measured to understand the up-conversion process under 808nm excitation. As shown in Fig. 5, the fitted slopes are 1.79 and 1.90 for the green and red emissions in $NaYF_4$:0.5 mol% Er^{3+}, 14 mol% Yb^{3+}, which comes to be 1.88 and 1.91 for $NaYF_4$:5 mol% Er^{3+}, 14 mol% Yb^{3+} respectively, indicating that the two emissions at two different Er^{3+} concentrations both exhibit two-photon processes.

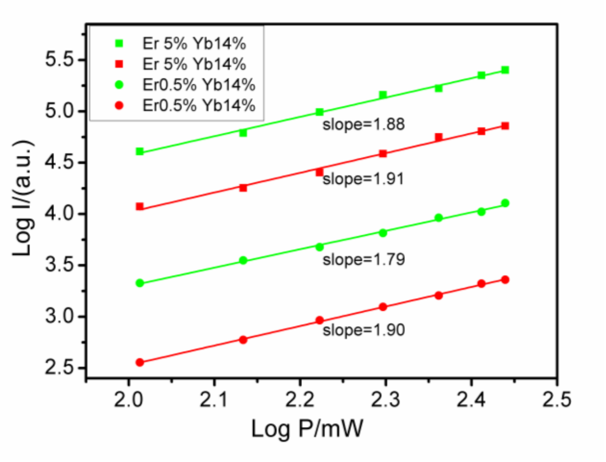

Fig. 5. Double-logarithmic plots of pump power dependence of green and red emissions for the samples of $NaYF_4$:0.5 mol% Er^{3+}, 14 mol% Yb^{3+} and $NaYF_4$:5 mol% Er^{3+}, 14 mol% Yb^{3+}.

In order to explain the Yb^{3+} dependent up-conversion behavior at different Er^{3+} concentrations, possible energy transfer pathways between Er^{3+} and Yb^{3+} are depicted in Fig. 6. For the samples with 0.5 mol% Er^{3+}, the introduction of Yb^{3+} drastically decreases the up-conversion emission due to the energy transfers from $Er^{3+} \rightarrow Yb^{3+}$. These energy transfers include ET (1) $^4I_{11/2}$ (Er^{3+}) + $^2F_{7/2}$ (Yb^{3+}) → $^4I_{15/2}$ (Er^{3+}) + $^2F_{5/2}$ (Yb^{3+}), ET (2) $^2H_{11/2}$ / $^4S_{3/2}$ (Er^{3+}) + $^2F_{7/2}$ (Yb^{3+}) → $^4I_{11/2}$ (Er^{3+}) + $^2F_{5/2}$ (Yb^{3+}) [32, 33]. However, with Yb^{3+} concentration increasing from 5 mol% to 14 mol%, both the green and red emissions slightly increase, just as shown in Fig. 4. Thus it is speculated that a no-resonant energy transfer, i.e., ET (3) $^4I_{9/2}$ (Er^{3+}) + $^2F_{7/2}$ (Yb^{3+}) → $^4I_{15/2}$ (Er^{3+}) + $^2F_{5/2}$ (Yb^{3+}), might also take place, exciting Yb^{3+} ions into their excited states. With the increase of population at Yb^{3+} excited state, the subsequent back energy transfer including BET (1) $^4I_{15/2}$ (Er^{3+}) + $^2F_{5/2}$ (Yb^{3+}) → $^4I_{11/2}$ (Er^{3+}) + $^2F_{7/2}$ (Yb^{3+}) and BET (2) $^4I_{11/2}$ (Er^{3+}) + $^2F_{5/2}$ (Yb^{3+}) → $^4F_{7/2}$ (Er^{3+}) + $^2F_{7/2}$ (Yb^{3+}) improve the up-conversion. However, the transfer ET (3) in the low Er^{3+} concentration (0.5 mol%) samples is not efficient. Correspondingly the back energy transfers BET (1) and BET (2) can't significantly enhance the up-conversion. As a result, the quenching effect is dominant with the introduction of Yb^{3+} for the low-Er^{3+}-concentration samples.

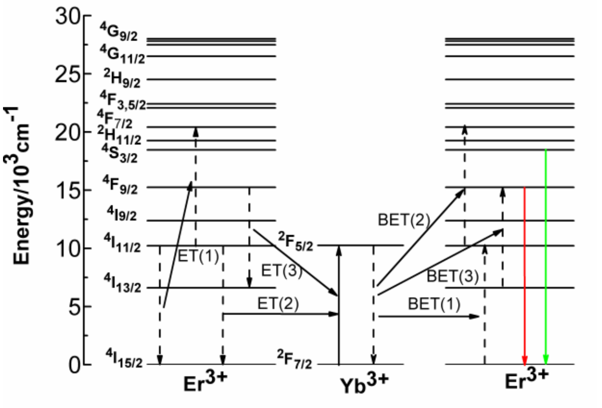

Fig. 6. Proposed up-conversion mechanism of $NaYF_4$:Yb^{3+}, Er^{3+} under 808 nm excitation.

For the samples with 5 mol% Er^{3+}, the increased Er^{3+} concentration further shortens the distance between Yb^{3+} and Er^{3+} ions. Consequently both the energy transfer ET (3) and back energy transfer BET (1) and BET (2) will be effectively enhanced. BET (2) is especially efficient owing to its excellent energy-level-matching performance. This leads to significant and continued enhancement of the green emission with Yb^{3+} concentration increasing from 0 to 14 mol%. As for the red emission, it is determined by the population of the $^4F_{9/2}$ level. The $^4F_{9/2}$ level is mainly populated by energy transfer between Er^{3+} ions for Er^{3+} singly doped sample, i.e., $^4I_{11/2}$ (Er^{3+}) + $^4I_{9/2}$ (Er^{3+})→ $^4I_{13/2}$ (Er^{3+}) + $^4F_{9/2}$ (Er^{3+}) [34]. With Yb^{3+} concentration increasing, the ET (1) will depopulate the $^4I_{9/2}$ level. This restrains the Er^{3+}- Er^{3+} energy transfer since it relies on the population density of Er^{3+} at $^4I_{9/2}$ state. Consequently, the population density of Er^{3+} at $^4F_{9/2}$ state also declines. Therefore, with Yb^{3+} concentration increasing from 0 to 8 mol%, the red emission is gradually weakened. However, at higher Yb^{3+} concentration, Another no-resonant back energy transfer BET (3) $^4I_{13/2}$ (Er^{3+}) + $^2F_{5/2}$ (Yb^{3+}) → $^4F_{9/2}$ (Er^{3+}) + $^2F_{7/2}$ (Yb^{3+}) is also intensified because of the increased Yb^{3+} ions at $^2F_{5/2}$ state. This back energy transfer increases the population of the $^4F_{9/2}$ level of Er^{3+}, enhancing the red emission. As a result, the red emission for 14 mol% Yb^{3+} co-doped sample is even twice stronger than that of Er^{3+} singly doped one. It is noted that Yb^{3+}-Yb^{3+} quenching will take place when Yb^{3+} concentration is too high. Therefore, both the green and red emissions begin to decrease at Yb^{3+} concentration of 17 mol%.

4. Conclusions

In conclusion, the effect of Yb^{3+} concentration on Er^{3+} up-conversion is investigated in $NaYF_4$:Yb^{3+}/Er^{3+}. Yb^{3+} decreases Er^{3+} up-conversion emission at low Er^{3+} concentration, while enhances the Er^{3+} up-conversion greatly at relatively high Er^{3+} concentration. A competitive energy transfer mechanism between Yb^{3+} → Er^{3+} and Er^{3+} → Yb^{3+} is proposed to explain the Yb^{3+}-codoping effect. The investigation offers a new way to enhance the near-infrared (808nm) to green (542 nm) and red (655 nm) up-conversion of Er^{3+} ions.

Acknowledgements

The work is supported by Scientific Research Fund of Hunan Provincial Educational Department (No. 10A120, 11B117), Hunan Provincial Natural Science Foundation of China (No.10JJ6012).

References

[1] A. Francois, Chem. Rev. **104**, 139 (2004).
[2] M. Haase, H. Schäfer, Angew. Chem. Int. Ed. **50**, 5808 (2011).
[3] F. Wang, X. G. Liu, Chem.Soc.Rev. **38**, 976 (2009).
[4] G. Poirier, F. C. Cassanjes, C. B. de Araujo, V. A. Jerez, S. J. L. Ribeiro, Y. Messaddeq, M. Poulain, J. Appl. Phys. **93**, 3259 (2003).
[5] B. C. Collings, A. J. Silversmith, J. Lumin. **62**, 271 (1994).
[6] X. F. Wang, S. G. Xiao, Y. Y. Bu, X. L. Yang, J. W. Ding, J. Lumin. **129**, 325 (2009).
[7] G. S. Maciel, A. Biswas, P. N. Prasad, Opt. Communications. **178**, 65 (2000).
[8] H. Scheife, G. Huber, E. Heumann, S. Bär, E. Osiac, Opt. Mater. **26**, 365 (2004).
[9] N. Rakov, G. S. Maciel, C. B. de Araujo, Y. Messaddeq, J. Appl. Phys. **91**, 1272 (2002).
[10] H. Fujiwara, K. Sasaki, J. Appl. Phys. **86**, 2385 (1999).
[11] D. Y. Wang, Y. Min, S. D. Xia, V. N. Makhov, N. M. Khaidukov, J. C. Krupa, J. Alloys Compd. **361**, 294 (2003).
[12] D. C. Yeh, W. A. Sibley, M. J. Suscavage, J. Appl. Phys. **63**, 4644 (1988).
[13] R. Naccache, F. Vetrone, V. Mahalingam, L. A. Cuccia, J. A. Capobianco, Chem. Mater. **21**, 717 (2009).
[14] H. Guo, Y. F. Li, D. Y. Wang, W. P. Zhang, M. Yin, L. R. Lou, S. D. Xia, J. Alloys Compd. **376**, 23 (2004).
[15] R. Weber, S. Hampton, P. C. Nordine, T. Key, R. Scheunemann, J. Appl. Phys. **98**, 043521 (2005).
[16] R. Balda, S. García-Revilla, J. Fernández, V. Seznec, V. Nazabal, X. H. Zhang, J. L. Adam, M. Allix, G. Matzen, Opt. Mater. **31**, 760 (2009).
[17] L. L. Xu, Y. N. Yu, X. G. Li, G. Somesfalean, Y. G. Zhang, H. Gao, Z. G. Zhang, Opt. Mater. **30**, 1284 (2008).
[18] T. Catunda, L. A. O. Nunes, A. Florez, Y. Messaddeq, M. A. Aegerter, Phys. Rev. B **53**, 6065 (1996).
[19] X. F. Wang, X. H. Yan, Opt. Lett., **36**, 4353 (2011).
[20] S. R. Bullock, B. R. Reddy, P. Venkateswarlu, S. K. Nash-Stevenson, J. C. Fajardo, Opt. Quantum Electron. **29**, 83 (1997).
[21] W. L. Lu, L. H. Cheng, H. Y. Zhong, J. S. Sun, J. Wan, Y. Tian, B. J. Chen, J. Phys. D: Appl. Phys. **43**, 085404 (2010).
[22] Y. H. Wang, J. Ohwaki, Appl. Phys. Lett. **63**, 3268 (1993).
[23] M. P. Hehlen, N. J. Cockroft, T. R. Gosnell, A. J.Bruce, Phys. Rev. B **56**, 9302 (1997).
[24] J. F. Suyver, J. Grimm, M. K. van Veen, D. Biner, K. W. Krämer, H. U. Güdel, J. Lumin. **117**, 1 (2006).
[25] G. S. Yi, H. C. Lu, S. Y. Zhao, Y. Ge, W. J. Yang, D. P Chen, L. H. Guo, Nano letters **4**, 2191 (2004).
[26] S. Inoue, A. Nukui, K. Sog, A. Makishima, J. Am. Ceram. Soc. **77**, 2433 (1994).
[27] Y. Y. Bu, S. G. Xiao, X. F. Wang, W. H. Yuan, J. W. Ding, J. Lumin. **130**, 38 (2010).
[28] X. F. Wang, S. G. Xiao, X. L. Yang, J. W. Ding, J. Mater Sci. **43**, 1354 (2008).
[29] Z. Pan, S. H. Morgan, J. Lumin. **75**, 301 (1997).
[30] M. Shojiya, M. Takahashi, R. Kanno, Y. Kawamoto K. Kadono, Appl. Phys. Lett. **65**, 1874 (1994).
[31] T. Danger, J. Koetke, R. Brede, E. Heumann, G. Huber, B. H. T. Chai, J. Appl. Phys. **76**, 1413 (1994).
[32] A. S. Oliveira, M. T. de Araujo, A. S. Gouveia-Neto, A. S. B. Sombra, J. A. Medeiros Neto, N. Aranha, J. Appl. Phys. **83**, 604 (1998).
[33] P. V. Dos Santos, M. T. de Araujo, A. S. Gouveia-Neto, J. A. Medeiros Neto, A. S. B. Sombra, Appl. Phys. Lett. **73**, 578 (1998).
[34] F. Vetrone, J. C. Boyer, J. A. Capobianco, J. Phys. Chem. B **107**, 10747 (2003).

---

[*] Corresponding author: xiaosiguo@xtu.edu.cn